THE JOURNAL OF PHYSICAL CHEMISTRY B

Article

pubs.acs.org/JPCB

Local Structure of Si-Al-Ca-Na-O Glasses from Coupled Neutron and X-ray Total Scattering Data

Andrea Bernasconi,[†] Monica Dapiaggi,*[,†] Alessandro Pavese,[†] Daniel T. Bowron,[‡] and Silvia Imberti[‡]

[†]Dipartimento di Scienze della Terra, Universitá degli Studi di Milano, Milano, Italy

[‡]ISIS Facility, Rutherford Appleton Laboratory, Didcot, OXON, OX11 0QX, United Kingdom

ABSTRACT: Amorphous materials became significantly important and more widely studied during the last few decades, due the their increasingly widespread applications in materials science and technology. Their local structure seems to have a very strong bond with those properties: in this paper, the local structure of Si-Al-Ca-Na-O glasses is studied by means of total scattering. EPSR simulations, coupling neutron, and X-ray data have been used to study glass samples (as a function of composition), with a composition close to the one used in their technological applications (ceramic glazes), providing a consistent structural model. The disordered structure of these materials has been evaluated in terms of network-forming/modifier elements. The network-forming elements (silicon and aluminum) show coordination numbers and bond angles that are consistent with a tetrahedral arrangement. In contrast, network-modifying elements (Ca and Na, whose content is different in all samples) depolymerize the network, increasing the number of nonbridging oxygens. This structural information is required to rationalize many important technological properties of these materials, such as the glass transition temperatures and thermal expansion, that control their efficiency as glazes.

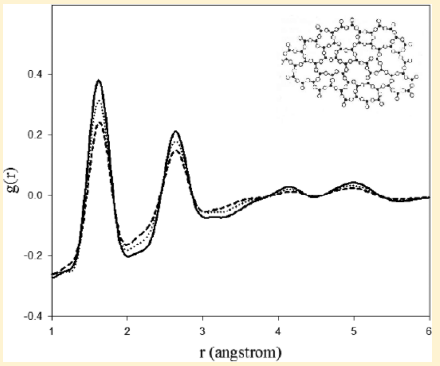

INTRODUCTION

Amorphous materials are increasingly important in the last decades, as many functional materials and many dielectrics are either nanocrystalline or amorphous (see ref 1 for a review). In ceramic production, an amorphous component is almost always present and has gained a lot of attention because the macroscopic properties of the ceramic bodies seem to be strongly related to its characteristics (namely, its chemical composition as well as the features of its local structure). In particular, our interest is focused on the amorphous component of the glazes that cover the ceramic bodies on large sanitaryware. They are usually deposited as a raw mixture on the surface of the ceramic body before heating. These coatings serve more than just an aesthetic role and have to fulfill certain technological characteristics. In particular, the coatings have to perfectly adhere to the underlying material, they have to expand (during heating) and to shrink (during cooling) in exactly the same way as the ceramic body in order to avoid the formation of surface cracks, and they must provide chemical and moisture resistance to the objects they coat. Control of these characteristics is usually addressed by varying the chemical composition of the starting mixture, which usually contains a complex mixture of silicon, aluminum, calcium, sodium, magnesium, zinc, potassium, and oxygen, together with a certain amount (usually less than 10 wt %) of zircon ($ZrSiO_4$), which is frequently added to make the coating opaque.[2] Variations in thermal expansion are usually ascribed to the strength of chemical bonding, which, in turn, depends on composition and structure.[3] Variation of the atoms involved in the chemical bonding, of the coordination number in the polyhedra, or of the angle between the atoms involved in the atomic network, may influence the flexibility of chemical bonds and, therefore, the amplitude of thermal vibration.[4] Previous works investigating these materials were largely focused on the glass transition temperature that is related to the grade of polymerization of the network, and that is influenced by the corner-sharing of Si and/or Al tetrahedra.[5,6]

Because of their intrinsic disorder, yet generally homogeneous chemical composition, the structure of these materials cannot be studied in the same way as long-range ordered crystalline materials. A different approach focusing on their local structure is needed. Molecular dynamics calculations or Monte Carlo simulation are a widely used approach to understanding the myriad of interatomic structural properties of the system, but these methods suffer from the limitation that their results will only reflect the prior assumptions made in the choice of interatomic interaction potentials. Experimentally, one can access real structural information by means of a total scattering experiment,[7] X-ray absorption fine structure spectroscopy (EXAFS, see ref 8, for example), or again nuclear magnetic resonance (NMR, see ref 9, for example), but this data is often complicated by the $N(N + 1)/2$ pairwise interactions, or subset of interactions, between the number of atomic species, N, that contribute to the measured experimental signals.

Received: July 6, 2012
Revised: October 5, 2012
Published: October 8, 2012

   dx.doi.org/10.1021/jp306697w | *J. Phys. Chem. B* 2012, 116, 13114−13123

Table 1. Chemical Composition of the Starting Materials Expressed as Oxide Weight Percentage and Atomic Fraction (AF)[a]

sample	silicon		aluminum		calcium		sodium		density
	SiO_2 (wt %)	AF	Al_2O_3 (wt %)	AF	CaO (wt %)	AF	Na_2O (wt %)	AF	(g cm^{-3})
A	74.24	0.25	12.37	0.05	7.53	0.04	5.86	0.04	2.49
B	69.62	0.23	11.60	0.04	7.06	0.03	11.72	0.08	2.56
C	65.01	0.21	10.83	0.04	6.59	0.03	17.57	0.12	2.62

[a]Note that the AF values have been directly adopted to obtain, for each element, the number of atoms to put in the simulating box.

This paper deals with structural information obtained by means of a combined neutron and X-ray total scattering experiment, analyzed using a Monte Carlo simulation that is constrained to evolve to achieve agreement with the available experimental data.[10] The effectiveness of such an approach to produce a realistic model of the glassy system is governed by the quality and the contrast to structural features in the complementary experimental data used to drive the modeling process. To obtain good real space resolution to distinguish between pairwise correlations between atoms of quite similar sizes, and to minimize Fourier transform artifacts, it is necessary to have scattering or X-ray spectroscopy data to high momentum transfer (Q at least larger than 20 $Å^{-1}$, but ideally larger than 30−35 $Å^{-1}$). This is generally beyond the capabilities of conventional lab-based diffractometers or X-ray absorption spectrometers, so large-scale facilities are usually required.[11] Synchrotron and neutron facilities (reactor or spallation source) also provide high flux radiation sources that minimize data collection times and allow for the collection of data with high statistical quality. A total scattering experiment produces an interference differential cross section or total structure factor, $F(Q)$, defined as eq 1

$$F(Q) = \sum_{\alpha\beta} (2 - \delta_{\alpha\beta}) c_\alpha c_\beta b_\alpha b_\beta [S_{\alpha\beta}(Q) - 1] \quad (1)$$

where c_α, c_β, b_α, and b_β are the atomic fractions and neutron scattering lengths of each type of atom in the sample, $\delta_{\alpha\beta}$ is the Kronecker δ function to avoid double counting the interactions between like species, and Q is the magnitude of the momentum transfer vector in the scattering process. The partial structure factors $[S_{\alpha\beta}(Q) - 1]$ are summed together (with c_α, c_β, b_α, and b_β weighting them), to give the total $F(Q)$ in eq 1). The partial structure factors are related to the partial pair distribution function $g(r)$ by a sine Fourier transform, as shown in eq 2)

$$g_{\alpha\beta}(r) - 1 = \frac{1}{(2\pi)^3 \rho} \int_0^\infty 4\pi Q^2 [S_{\alpha\beta}(Q) - 1] \frac{\sin Qr}{Qr} \, dQ \quad (2)$$

where ρ is the atomic density of the sample. Like the total structure factor $F(Q)$, the total pair distribution function $g(r)$ is simply the weighted sum of all the partial $g_{\alpha\beta}(r)$, described in eq 2. These functions describe the probability of an atom of type β to be in a coordination shell at a distance r from an atom of type α. A total scattering experiment is, therefore, able to provide, through the described functions, a description of the structure in an amorphous material.

The aim of this paper is to investigate the local structure of amorphous materials, in a selected compositional range. The wide chemical variability of sanitary glazes required an initial study and proof of principle: a set of three glasses with simplified compositions were chosen for the investigation. The samples consist of systems with a fixed compositional ratio of Si, Al, Ca, and O, with varying contents of Na. It will be especially interesting to experimentally check the charge-compensating role (or network-modifier role) of Na and Ca, which is of seminal importance in understanding the relationship between structure and properties. This information can then be directly compared with the results obtained by means of EXAFS and molecular dynamics simulations,[12] and molecular dynamics only.[13] The experimental approach consists in coupling neutron with high-energy X-ray data. Neutron methods are particularly useful for investigating these materials as they have good sensitivity to light and very light elements.[14] To complement the neutron scattering data and to provide a second set of experimental constraints that are more sensitive to the contributions from the heavier elements in the materials, Ag Kα laboratory X-ray diffraction was used to measure a second total structure factor for each of the investigated glasses. These were then combined with neutron data in an EPSR (empirical potential structure refinement[15])-type model.

SAMPLE PREPARATION, DATA TREATMENT, AND MODELING

Sample Preparation. Three different Si-Al-Ca-Na-O glasses have been investigated in the present work. As in the industrial practice, the SiO_2/Al_2O_3 ratio has been fixed to 6 with various amounts of Na_2O. This approach will allow us to check for the influence of this cation on the local structure of our samples (nominal Na_2O contents were 6, 12, and 18 wt %). The calcium amount is about 7 wt %; aluminum and silicon oxide contents were added to reach 100%. To achieve the desired composition, the appropriate amounts of different reagents (quartz SiO_2 from Sigma-Aldrich (purum, ≥95%), alumina Al_2O_3 from Sigma-Aldrich (99.7%), calcium oxide CaO from Analar (99.5%), and sodium carbonate Na_2CO_3 from Analar (99.9%)) have been carefully weighed and then mixed together in an agate mortar. Each raw mixture was then heated to 1200 °C in a platinum crucible and kept at this temperature for 20 min. Once melted, the whole platinum crucible was quenched in cold water to obtain an amorphous material. X-ray powder diffraction measurements, performed with a laboratory PANalytical X′ Pert Pro diffractometer, showed that all three samples did not contain any crystalline phase. The chemical composition of the glass samples is shown in Table 1. Density measurements have been performed with a Quantachrome micropycnometer, because this information is important for the preliminary data treatment and for the EPSR modeling: results can be found in Table 1.

Neutron and X-ray Data Collection and Treatment. Neutron diffraction data were collected over a wavelength range of 0.05−4.95 Å at the SANDALS diffractometer, providing access to the glass total structure factor scattering vector (Q) ranges from 0.2 to 50 $Å^{-1}$. Powdered samples were manually pressed into flat TiZr alloy (packing fraction of 0.481 and density of 0.0542 atoms $Å^{-3}$) cans, with a diameter of 35 mm and with walls with a thickness of 1 mm. Each sample has

been measured for at least 9 h to obtain a good signal-to-noise ratio; then additional shorter measurements (3−6 h) have been performed on an empty instrument (3 h), vanadium reference (6 h), and all the empty cans (3−6 h). Complementary data have been obtained on a Ag Kα (wavelength = 0.559 Å) PANalytical X-Pert Pro laboratory X-ray diffractometer, equipped with a scintillation detector, available in the ISIS second target station support laboratories. Data were collected for 48 h over a Q range of 0.65−20 Å^{-1}.

Both the neutron and the X-ray scattering data have to be normalized and background (from instrument and sample holder) corrected before they can be Fourier transformed to a pair distribution function. In both cases, the GUDRUN[16] software was used to perform the necessary normalizations and corrections.

Data Modeling. Data have been modeled using EPSR (empirical potential structure refinement).[10,17] Each glass model consisted of a cubic box with periodic boundary conditions containing 1700 atoms, sized to match the measured glass density of 0.0542 atoms Å^{-3}. EPSR starts from a standard Monte Carlo (MC) simulation that moves atoms, or molecules, by means of translations and rotations. A move consists of a small change in the (x,y,z) coordinates of atoms and molecules, and the acceptance of this move is based on the Metropolis condition, which compares the potential energy before and after the move.

The first step in EPSR is to perform standard MC runs with the reference potentials only. Once the system reaches equilibrium, the structure factors of the model are calculated and compared to those obtained from scattering data. This difference between model and experiment is then used to generate a set of empirical potential perturbation functions that are added to the reference potential in the next step of the method, with the aim of driving the model into agreement with the experimental data. This procedure of calculating the difference between the experimental and model structure factors, generating a perturbation potential to modify the atomic interactions, is continued until, at the end of the process, the pairwise distribution of atoms in the model agrees with the experimental structure factors. Once the model (and underlying empirical potential) has converged, the Monte Carlo process is continued and average structure functions are calculated. These provide access to the desired information about atomic correlations.

In EPSR, the reference potential between two atoms ij, whose chemical nature is described by α and β, is calculated on the basis of a two-body Lennard-Jones potential, plus effective Coulomb charges, as expressed by eq 3

$$U_{\alpha\beta}(r_{ij}) = 4\varepsilon_{\alpha\beta}\left(\left(\frac{\sigma_{\alpha\beta}}{r_{ij}}\right)^{12} - \left(\frac{\sigma_{\alpha\beta}}{r_{ij}}\right)^{6}\right) + \frac{q_\alpha q_\beta}{4\pi\varepsilon_0 r_{ij}} \quad (3)$$

where $\varepsilon_{\alpha\beta}$ is the well depth parameter, $\sigma_{\alpha\beta}$ is the range parameter, r_{ij} is the distance between the atoms, and $q_\alpha q_\beta$ are the formal Coulomb charges of the α and β species. Table 2 reports the adopted values of ε, σ, and ionic charges for the various atom species. $\varepsilon_{\alpha\beta}$ and $\sigma_{\alpha\beta}$ can be calculated from the values in Table 2 by means of the Lorentz−Berthelot mixing rules.

The reference potentials provide stringent primary constraints on the generated models since the empirical potential generated from the data is designed to operate best as a small perturbation on this interaction baseline. Silicon and oxygen data in Table 2 were taken directly from the literature.[7] The reference parameters for the other elements in the glass were chosen to deliver appropriate first neighbor distance interactions and charge-balanced local stoichiometries that were consistent with the adopted silica parameters. This is an important consideration when setting up the reference potential model of a network glass since the empirical potential generated in the analysis is not capable of overcoming major discrepancies if the reference potential favors first neighbor contacts at too great an interaction distance. Aluminum environments were expected to be close to those of silicon due to the similarities in the behavior of the two elements, regarding both coordination number and bond distance with oxygen.[18] Things were a little more complex for sodium and calcium, as both Na−O and Ca−O distances range from 2.1 to 2.6 Å, in alumino-silicate glasses.[8,9,12,19,20] The experimentally derived total pair distribution functions, $g(r)$, show two peaks in this range (see Figure 1), the first one attributed to Ca−O and Na−O bond distances, and the second one to O−O bond distances. This choice can be better explained with a comparison among the experimental $g(r)$ of our three samples (Figure 1): a decrease in intensity of the 1.6 Å peak and an increase in intensity of the 2.2 Å peak in $g(r)$ from sample A to sample C can be addressed to the variations in the samples' chemical composition. In fact, sample A, characterized by the highest content of Si and Al, has the most intense 1.6 Å peak in $g(r)$; on the other hand, sample C, characterized by the highest content of Na, has the highest 2.2 Å intensity in $g(r)$. After a few preliminary tries, σ values for Ca and Na were fixed to 2.2 Å and 2.8 Å, respectively. Following equilibration with these parameters, sample C exhibits the graphical fit (dotted line) shown in Figure 2, where the left-hand panel represents the fit to the neutron data and the right-hand panel to the X-ray data.

Table 2. Configuration and Final Lennard-Jones Parameters

atom	ε (kJ mol^{-1})	σ (Å)	q (e)
Si	0.80	0.76	+4
Al	0.80	1.20	+3
Ca	0.80	2.20	+2
Na	0.80	2.30	+1
O	0.65	3.69	−2

By looking at the residuals, one can note that the larger differences can be found around 2.2 Å (underestimation of the calculated intensity) and around 2.6 Å (overestimation of the calculated intensity). With a σ value for sodium of 2.8 Å, its partial $g(r)$ shows the first peak at 2.6 Å, likely producing the overestimation of the calculated intensity in this range. If we now reduce the sodium σ value to 2.3 Å, the first peak of the partial $g(r)$ for Na−O distance moves to 2.3 Å, giving a much better fit (see dashed line in Figure 2) and a Na−O distance more consistent with the literature data.[12,21] The final fits of $S(Q)$ and $g(r)$ of all three samples are shown in Figure 3.

RESULTS AND DISCUSSION

In this section, we have separated the results from EPSR modeling into different subsections according to the role of the atoms in the glass structure: network-forming elements, network modifiers, and oxygen-sharing properties.

Network-Forming Elements. Silicon and aluminum are network-forming elements, as they confer stability to the structure because of the interconnection of their local, largely

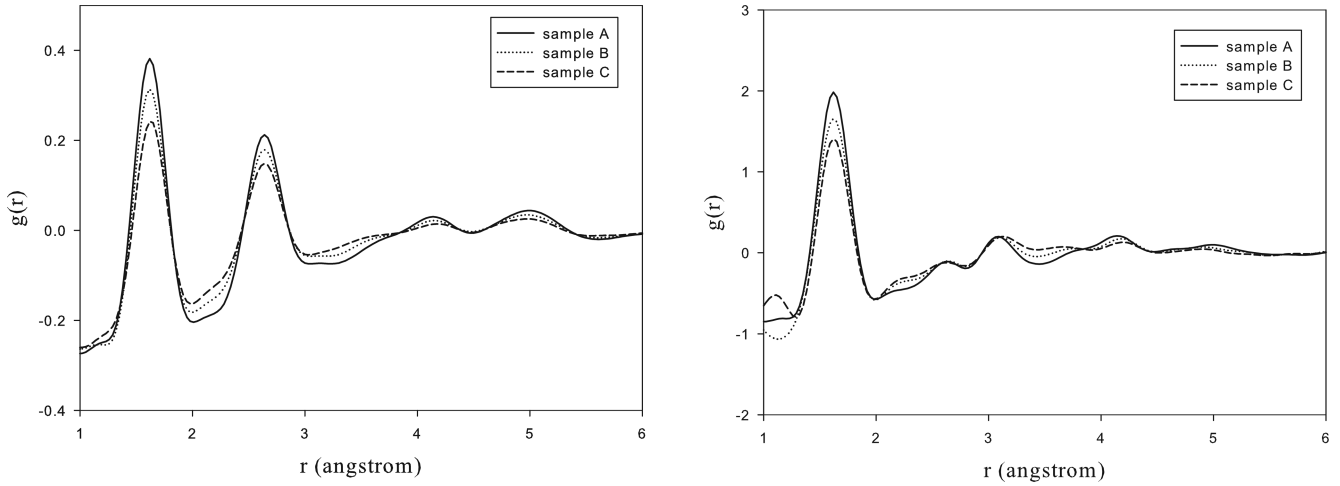

Figure 1. Comparison of the experimentally measured total $g(r)$'s for the three samples investigated. Neutron data are on the left-hand side, X-ray data on the right-hand side.

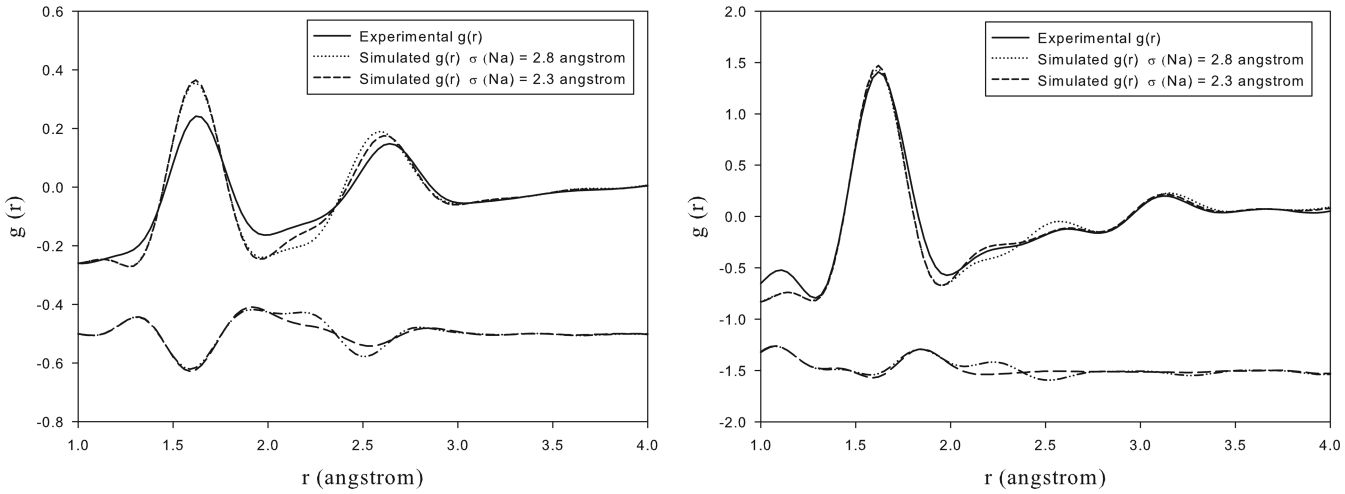

Figure 2. Real space illustration of the misfit at 2.2 Å getting better as the reference potential parameters are optimized prior to EPSR refinement. Neutron data are on the left-hand side, X-ray data on the right-hand side.

tetrahedral, structural units. In all three samples, the Si−O partial pair distribution function has the first peak at about 1.62 Å (see top part of Figure 4) without significant variations between samples. The calculated coordination number distributions for silicon (middle part of Figure 4) confirm the well-defined structural environment of silicon. In all three samples, a fraction of 0.99 of silicon atoms have a 4-fold coordination. Furthermore, in all three samples, the most probable O−Si−O angular value (107°30′) is close to the ideal tetrahedral value of 109°47′. Bond distances, evaluated from the maximum of the peak in the corresponding partial $g(r)$, for network-forming elements, can be found in Table 3. In the same table, the O−M−O angles are taken from the peak maximum in the probability distributions shown in the bottom part of Figure 4; the values in parentheses represent the full width at half-maximum (fwhm) of the probability distributions, as a measure of the disorder in the angular values. As it can be seen from Table 3, an increase in sodium content, from sample A to sample C, seems to sharpen the O−Al−O distribution (fwhm goes from 23.5 to 16.5 with increasing Na content) and, on the other hand, to widen, though in a less distinct way, the O−Si−O distribution (fwhm goes from 14.8 to 16.5 with increasing Na content). The coordination numbers shown in Table 3 are the average values of the frequency histograms shown in Figure 4, while the numbers in parentheses represent the distance from the corresponding average value. The first significant difference in the short-range order can be noted in Table 3 for aluminum atoms, as also shown by the different position of the first peak in the partial $g(r)$ for the Al−O bond (see top part of Figure 4) and by the different coordination number of aluminum (see middle part of Figure 4). In fact, when the sodium content is increased from sample A to sample C, the aluminum average coordination number moves from 3.64 to 3.89, as shown in the middle part of Figure 4. However, the distortion of the coordination polyhedra seems to be inversely related to the sodium content, as shown by the wider O−Al−O angular spread (bottom part of Figure 4). No evidence of five-coordinated Al sites has been obtained with these simulations. All of these results are in agreement with previous works on a similar glass composition.[5] The presence of Al in tetrahedral sites with oxygen atoms at the vertices of the geometric unit produces a lack in positive charge that is compensated by mono- or bivalent ions (Ca and Na), making the Al−Ca and Al−Na distances shorter than the corresponding distances for Si, as will be seen in more detail in the next section.

dx.doi.org/10.1021/jp306697w | J. Phys. Chem. B 2012, 116, 13114−13123

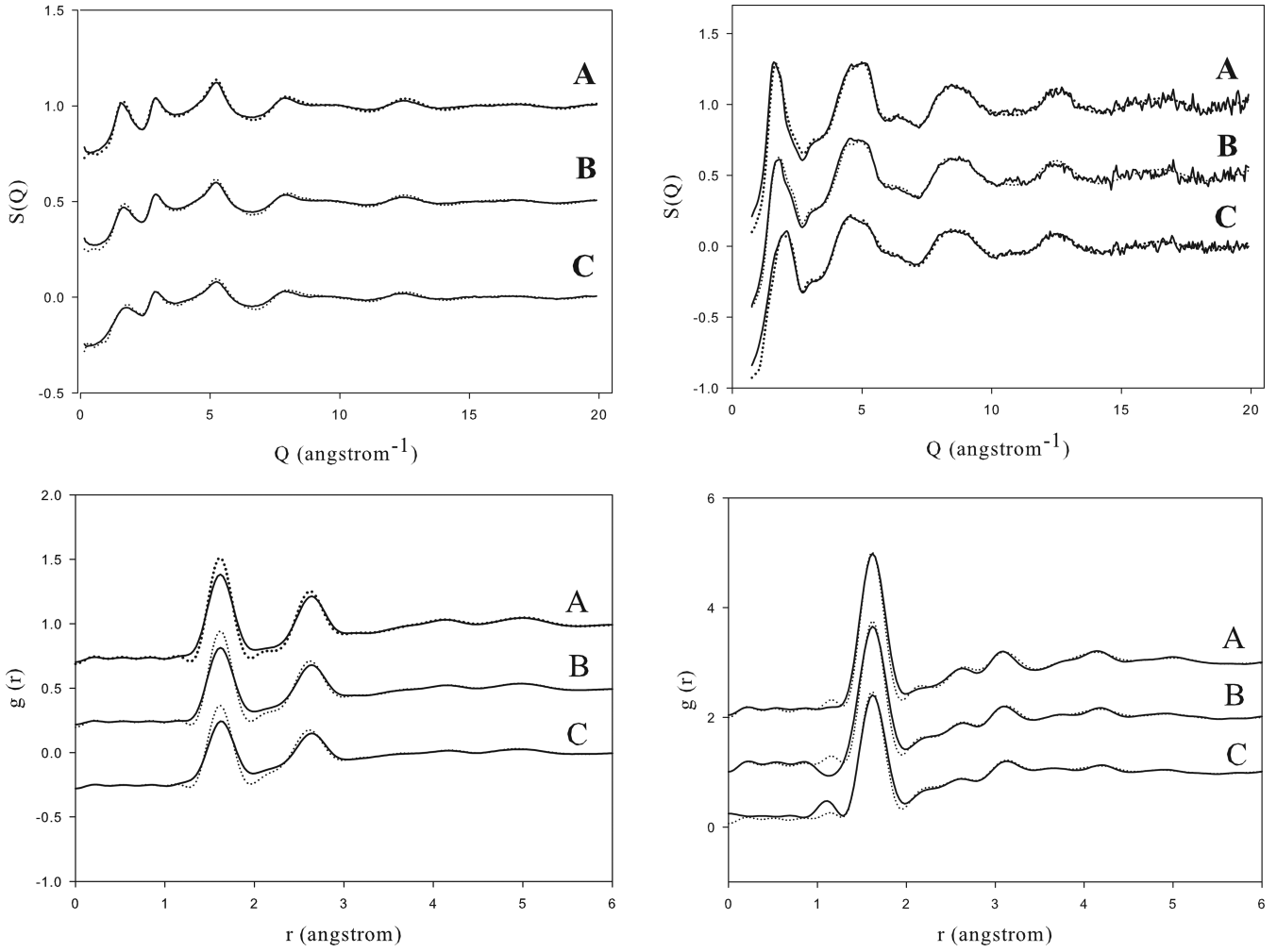

Figure 3. Final total $F(Q)$ EPSR fits to the neutron (left-hand side) and X-ray (right-hand side) data. The EPSR model was only refined against the $F(Q)$ data to avoid the risk of fitting Fourier transform artifacts in the total pair distribution functions. However, for completeness, the resulting comparison in real space is also shown in the lower panels.

Network-Modifying Elements. Calcium and sodium atoms can play two different roles in aluminosilicate glasses. They can be network-modifying elements that depolymerize the network, but they can also, as previously mentioned, have a charge-compensating effect when they are adjacent to AlO_4^- tetrahedra. For Ca and Na, the choice of the cutoff values to be used in order to obtain reasonable values for distances, coordination numbers, and O−M−O angular values, is crucial and particularly delicate. In fact, by looking at the top part of Figure 5, one can easily see that the partial $g(r)$ for Ca−O and Na−O is not as sharp as that for Si−O and Al−O, and the peaks show intensity spreading from the peak to larger distances. Because of this, different cutoff choices may produce slightly different values for Ca−O and Na−O coordination numbers and average distances. However, this does not produce a "wrong" value for the values that are determined, but care must be taken if these values are to be compared with other literature values that may have used different criteria, and as remarked by Zotov and Keppler.[21] For this reason, in this study, we have used the same cutoff value for all the samples, in order to obtain comparable results. This fixed criteria also applies to the quoted values for coordination numbers (see middle part of Figure 5) and for O−M−O angular distributions (see bottom part of Figure 5).

The Ca−O bond distance observed in our structural models is around 2.2 Å in all three samples (see Table 4), and the Ca coordination number does not change much between samples, with mean values ranging from 5.02 to 5.08 (in agreement with Cormier et al.[6]), with increasing sodium content. The large spread in coordination number (from 3 to 7, as seen in the middle part of Figure 5) indicates that calcium has a disordered distribution in the structure, without a well-defined coordination polyhedron. This consideration is confirmed by the O−Ca−O angular distribution, with angles varying from 60 to 180° (see bottom part of Figure 5, and Figure 4). By looking at Table 4, one can easily note the charge-compensating effect of Ca and Na for aluminum in tetrahedral coordination: Al−Ca and Al−Na distances are much smaller than Si−Ca and Si−Na distances: for instance, in sample A, Al−Ca and Al−Na distances are 2.88 and 3.00 Å, respectively, while Si−Ca and Si−Na distances are 3.40 and 3.45 Å, respectively.

Sodium has a behavior similar to the one of calcium. The first peak in the Na−O partial $g(r)$ is displaced to a smaller value from sample A to sample C: with increasing Na content, it goes from 2.4 to 2.29 Å, as also shown in Table 4 and visually in the top part of Figure 5, in agreement with the literature.[21] As for calcium, the comparison of the sodium coordination number with other works is not significant: our slightly different cutoff

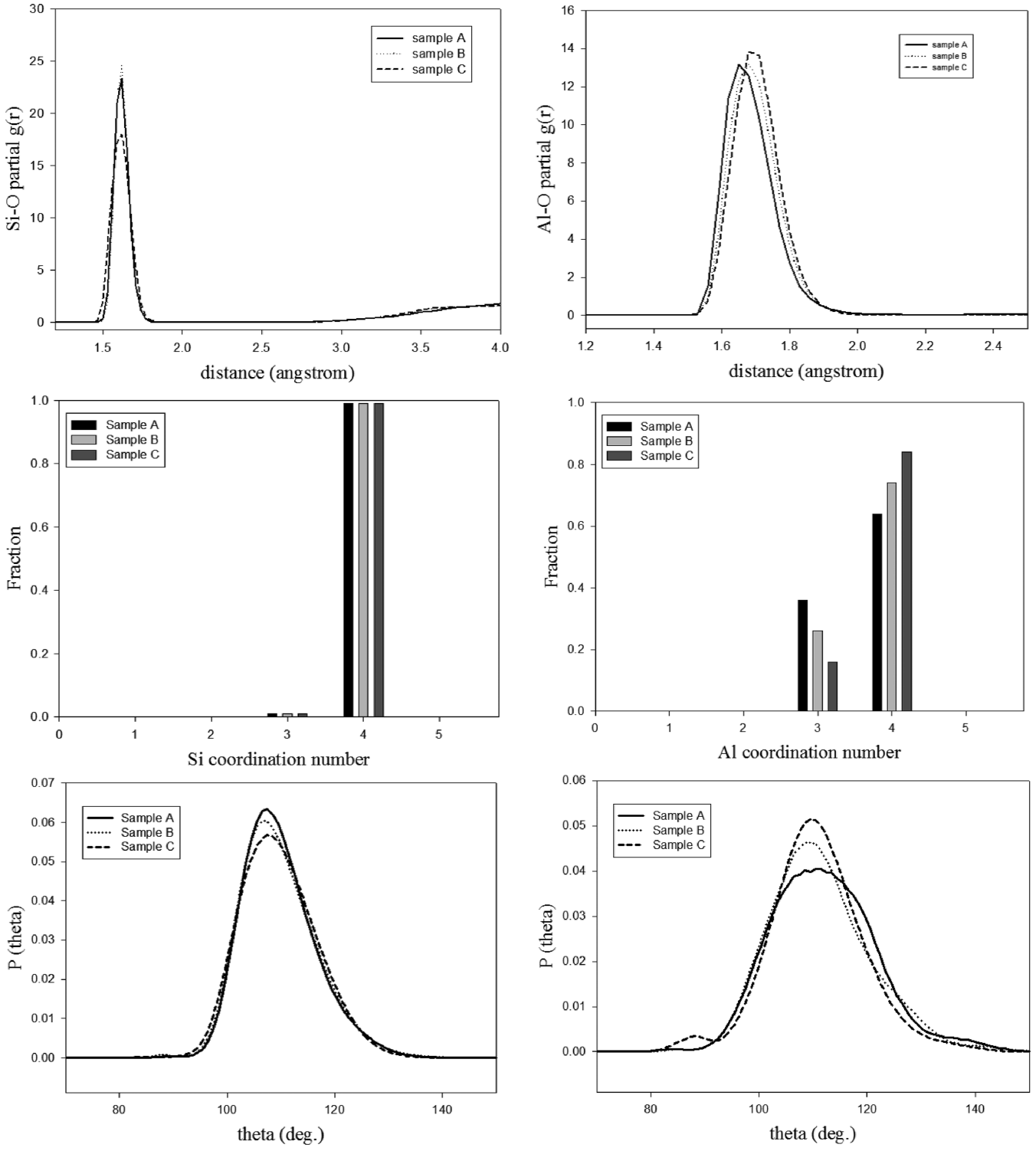

Figure 4. M−O partial $g(r)$, histogram of distribution of coordination number, and O−M−O angle distribution (M = Si on the left-hand side, M = Al on the right-hand side). A solid line represents data for sample A; a dotted line, those for sample B; and a dashed line, those for sample C.

value may easily explain our larger Na coordination number with respect to Zotov and Keppler.[21] As a matter of fact, sample C shows the smallest average Na coordination number (5.72), whereas a more diffuse coordination of 7−8 is present in sample A (middle part of Figure 5). Finally, the O−Na−O angular distribution is always wider than the O−Ca−O distribution and goes from about 45° to 180°, with two more pronounced peaks at about 55° and 85°(bottom part of Figure 5).

Bridging (BO) and Nonbridging (NBO) Oxygens. Data obtained with EPSR can also provide information about the type of oxygen bonding and sharing, such as, for example, the distribution of bridging oxygen (BO) and nonbridging oxygen (NBO). A simple computer code that interrogated the EPSR structural configurations of the investigated glasses allowed us

dx.doi.org/10.1021/jp306697w | J. Phys. Chem. B 2012, 116, 13114−13123

Table 3. Bond Distances, Coordination Numbers, and O−M−O Angles for Network-Forming Atoms[a]

	sample A	sample B	sample C
Si−O (Å)	1.62	1.62	1.62
Al−O (Å)	1.65	1.68	1.68
Si−O (coord no.)	3.99 (±0.09)	4.00 (±0.09)	4.00 (±0.08)
Al−O (coord no.)	3.64 (±0.48)	3.74 (±0.44)	3.89 (±0.37)
O−Si−O (angle)	107°30′ (14.8)	107°30′ (15.4)	107°30′ (16.5)
O−Al−O (angle)	111° (23.5)	107° (19.9)	109°30′ (16.5)

[a]The numbers in parentheses represent the distance from the average value. The cutoff values for Si−O distances were 1.45 and 1.9 Å, whereas those for Al−O distances were 1.45 and 2.1 Å. The numbers in parentheses after the angular values represent the full width at half-maximum of the peak in the probability distribution.

to distinguish between the various types of chemical and geometrical environments for the oxygen atoms. Before starting discussing the results, a few definitions follow. A bridging oxygen (BO) is defined as an oxygen that is shared by two tetrahedra in a sphere with a defined radius (the cutoff value used in this study was 2 Å); bridging oxygens were distinguished, in this work, by means of the type of polyhedra surrounding them. If one oxygen is shared by only two tetrahedra, it is called a BO′, whereas, if it is shared also by a different polyhedron (e.g., an octahedron), it is called BO″. Obviously, BO is equal to the sum of BO′ and BO″. Moreover, it was also possible to study the different arranging of Si and Al atoms, that is, the way through which they are linked with bridging oxygens (for total BO, BO′, and BO″): Si−O−Si, Si−O−Al, and Al−O−Al. An NBO is an oxygen that is shared by one single tetrahedron, but it could also be connected to a different coordination polyhedron. Furthermore, we can also take into account oxygens shared by three tetrahedra (tricluster, TBO), by no tetrahedra (tetrahedron-free oxygen, TFO), or not bonded at all (free oxygens, here called simply FREEOX). All of these results can be found in Table 5, obtained in all samples by using the cutoff values for Si and Al shells fixed at 2 Å and the one for Ca and Na fixed at 3.2 Å . As mentioned in the case of coordination number and bond angles, it is important to remark that the final results are strongly affected by the cutoff value, especially for BO′ and BO″. The table is organized as follows: for each sample, the first column reports the number of BO′, BO″, NBO, FREEOX, TBO, and TFO, in terms of fractions of the total oxygen atoms. The second column reports, for BO′ and BO″, the different arranging of Si and Al atoms (Si−O−Si, Si−O−Al, Al−O−Al), normalized to the total number of BO′ and BO″, respectively. The last part of the table shows the same results for the total BO atoms.

With the aid of the computer code, it was also possible to have a closer look at the role of Ca and Na in the glass network, by counting the number of BO″ within a cutoff distance from Ca and Na. For each chemical species, then, it was possible to establish the fraction of Si−O−Si, Si−O−Al, and Al−O−Al connected with Na or Ca. These results can be found in Table 6, obtained with the same cutoff values as in Table 5. The first line of the table shows the ratio between Na and Ca in the simulation box. In a much similar way as in Table 5, for each sample, the first column shows the number of BO″ connected to Na and Ca, in terms of the fraction of the total number of BO″. The second column shows the different arranging of Si and Al atoms, normalized to the total number of BO″ type (bonded to Na or Ca, respectively).

BO″ are divided in three types (i.e., those connected to Si−O−Si, to Si−O−Al, and to Al−O−Al). For each of them, the proportion of Na and Ca atoms connected to them is also shown. The table also shows, in the first line, for an easier comparison, the ratio of Na and Ca atoms present in the simulation box for each sample.

In our samples, NBO and BO are the most important oxygen classes, because they provide important information about the role of some cations involved in the structure, in particular, the role of chemical elements, such as Ca and Na. NBOs are due to the role of these elements as network modifiers and tend to depolymerize the network, whereas, on the other hand, BOs are sensitive to the charge-compensating role of these elements. This is well-known in literature.[5] Important differences are present in the three samples. As expected, BO″ and NBO fractions increase with increasing Na content (i.e., from sample A, where, for instance, the BO″ fraction is equal to 0.26, to sample C, where the BO″ fraction is equal to 0.40), whereas BO′ and total BO decrease (in sample A, for instance, the BO′ fraction is equal to 0.46; in sample B, it is equal to 0.32; and in sample C, it is equal to 0.21), though not in a strictly proportional manner. In fact, the differences are larger by going from sample A to sample B, then by going from sample B to sample C, even if the variation in Na content in exactly the same. TBO fractions (i.e., tribonded oxygens) are very small in all the samples (0.01), in agreement with the literature,[22] as their formation (as well as the formation of 5-fold aluminum) is more likely in peraluminous glasses, with a molar ratio between modifiers and Al smaller than 1 (i.e., $n_{MOD}/n_{Al} < 1$, where n is the number of moles of modifiers (MOD) and aluminum (Al)), rather than in peralkaline glasses, such as samples A, B, and C, where, instead, n_{MOD}/n_{Al} is 1.9, 2.7 and 3.8, respectively. Concerning Si/Al arrangements, the Si−O−Si linkage is the most diffused, because of the high Si/Al ratio in all the samples, whereas the number of Al−O−Al linkages is very small, in agreement with the so-called "avoidance rule".[23] By looking more closely at Table 5, it can be easily noted that the Si−O−Si linkage is more diffused in BO′ atoms, and this preference increases, from a fraction of 0.74 to a fraction of 0.80, with increasing Na content. On the other hand, in all three samples, the proportion of Si−O−Al linkages is larger for BO″ than for BO′ atoms, probably due to the lack of ionic charge for the substitution of Si with Al atoms. By looking at the total number of BO atoms (bottom part of the table), one can note that the arrangement of Si and Al atoms does not change with Na content, because it is determined by the Si/Al starting ratio only: the values for Si−O−Si, Si−O−Al, and Al−O−Al fractions are about 0.70, 0.27, and 0.03, respectively. The different roles of Ca and Na can be assessed by looking at the results in Table 6. It is particularly interesting to look at the different arrangements of Si and Al atoms around BO″ atoms linked to Na and Ca: there are no trends as a function of Na content. It should be noted that the fraction of BO″ connected to sodium increases with Na content, but it is not only determined by the larger amount of Na present (Na/(Na + Ca)), as it is always larger than the fraction of Na atoms in the simulation box (cf. first line of the table). This effect is more visible for sample A with respect to the other samples (i.e., the difference between the fraction of BO″ connected to Na and Na/(Na + Ca) is 0.12 for sample A, and decreases to 0.03 for samples B and C). The smaller differences in samples B and C can be explained by the simultaneous decrease, from sample A to sample C, in the number of AlO_4^- tetrahedra and the

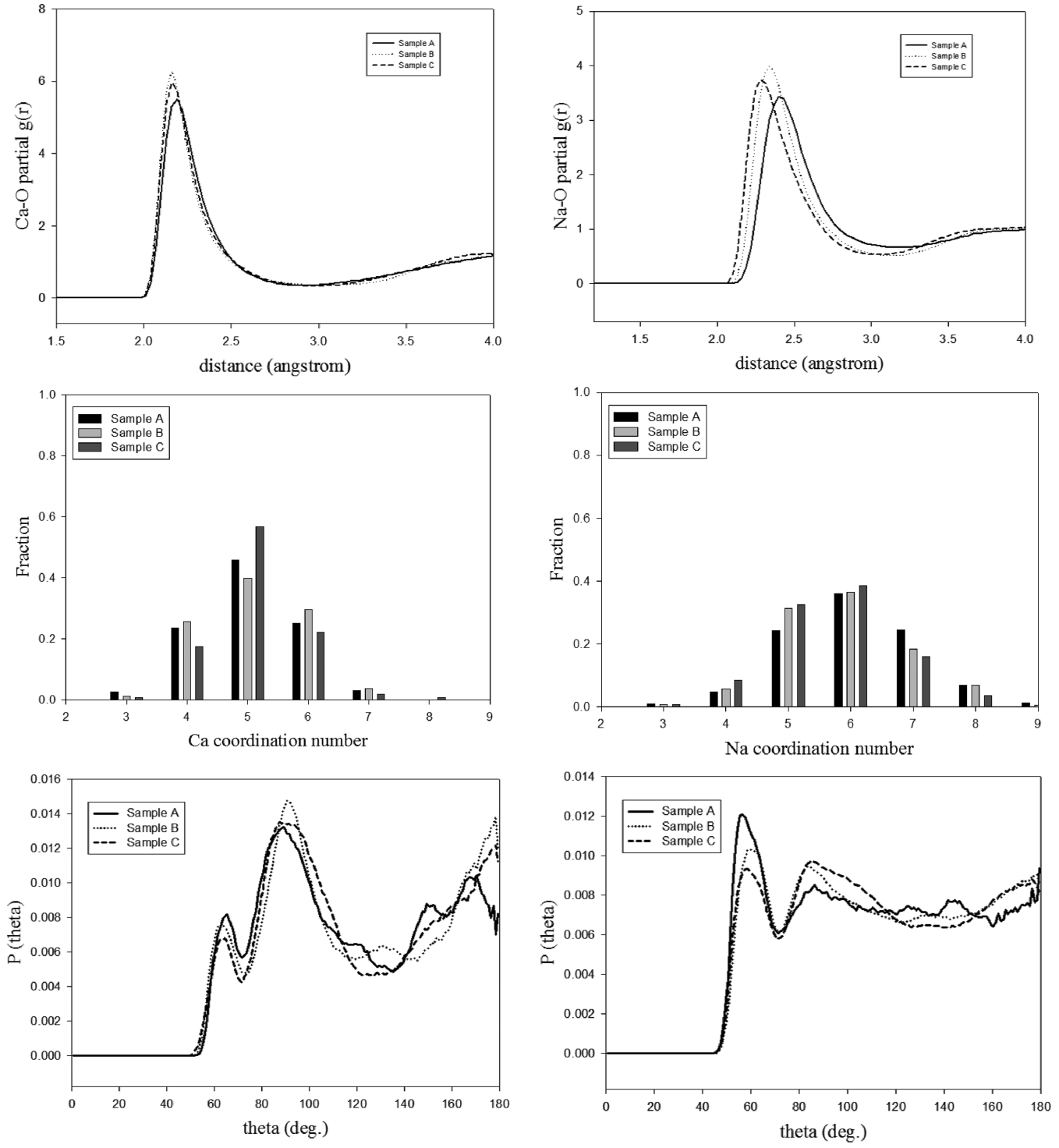

Figure 5. M−O partial $g(r)$, histogram of distribution of coordination number, and O−M−O angle distribution (M = Ca on the left-hand side, M = Na on the right-hand side). A solid line represents data for sample A; a dotted line, those for sample B; and a dashed line, those for sample C.

increase in the number of Na atoms: a lower number of negative charges needs to be balanced in the tetrahedra network, and the Na atoms tend to form a larger number of bonds with NBO. Moreover, the present paper showed that, due to a preference of Na atoms for BO″, well above the one due to the composition, there is a tendency for Na atoms to compensate the negative charge introduced in the tetrahedra by the presence of Al. A full comparison with the literature, such as with the papers by Cormier and Neuville[12] and by Cormack and Du,[13] which are the closest in composition to the samples studied here, is not trivial, because there are differences in both the chemical composition and the adopted cutoff values used for bond distances and angles. However, a few comments can be made, in particular, about the role of network modifiers: both cited papers find a larger number of NBOs around Ca atoms than around Na atoms, and this is compatible to what was found in this work (a preference of Na atoms for BO″). Furthermore, Cormier and Neuville[12] showed that, if sodium is

dx.doi.org/10.1021/jp306697w | J. Phys. Chem. B 2012, 116, 13114−13123

Table 4. Bond Distances, Coordination Numbers, and O−M−O Angles for Network-Forming Atoms[a]

	sample A	sample B	sample C
Ca−O (Å)	2.19	2.17	2.16
Na−O (Å)	2.40	2.34	2.29
Si−Ca (Å)	3.40	3.48	3.52
Si−Na (Å)	3.45	3.50	3.45
Al−Ca (Å)	2.88	2.90	2.90
Al−Na (Å)	3.00	2.92	2.90
Ca−O (coord no.)	5.03 (±0.84)	5.09 (±0.86)	5.10 (±0.75)
Na−O (coord no.)	6.00 (±1.17)	5.89 (±1.05)	5.72 (±0.99)
O−Ca−O (angle)	89°30′	91°	89°
O−Na−O (angle)	56°30′	60°	59°30′

[a]The numbers in parentheses represent the distance from the average value. The cutoff values for Ca−O distances were 1.9 and 2.9 Å, while those for Na−O distances were 2.0 and 3.2 Å.

Table 5. Distribution of Bridging and Nonbridging Oxygen Atoms[a]

	sample A		sample B		sample C	
BO′	0.46		0.32		0.21	
Si−O−Si		0.74		0.79		0.80
Si−O−Al		0.25		0.20		0.19
Al−O−Al		0.01		0.01		0.01
BO″	0.26		0.34		0.40	
Si−O−Si		0.62		0.61		0.63
Si−O−Al		0.35		0.33		0.32
Al−O−Al		0.03		0.06		0.05
NBO	0.25		0.31		0.35	
FREEOX	0.01		0.00		0.00	
TBO	0.01		0.01		0.01	
TFO	0.01		0.02		0.03	
BO	0.72		0.66		0.61	
(Si−O−Si)		0.70		0.70		0.70
(Si−O−Al)		0.28		0.27		0.27
(Al−O−Al)		0.02		0.03		0.03

[a]BO′ are oxygens shared only by two tetrahedra, BO″ are shared also by another polyhedron, NBO belongs to a single tetrahedron, FREEOX are not bonded, TBO are shared by three tetrahedra, and TFO are not linked to any tetrahedron (but to other polyhedra). BO is the total fraction of bridging oxygens (i.e., equal to the sum of BO′ and BO″). More details can be found in the text.

Table 6. Distribution of Bridging and Nonbridging Oxygen Atoms[a]

	sample A		sample B		sample C	
Na/(Na + Ca)	0.50		0.69		0.79	
BO″ (Na)	0.62		0.72		0.82	
Si−O−Si		0.67		0.59		0.64
Si−O−Al		0.30		0.34		0.31
Al−O−Al		0.03		0.07		0.05
BO″ (Ca)	0.38		0.28		0.18	
Si−O−Si		0.55		0.65		0.60
Si−O−Al		0.42		0.31		0.37
Al−O−Al		0.02		0.04		0.03

[a]BO″ are oxygens shared by two tetrahedra and by another polyhedron. More details can be found in the text.

replaced by calcium, and the molar ratio n_{MOD}/n_{Al} is 1.33, an almost fixed ratio between BO and NBO is observed; that is, a similar polymerization degree is likely in all the samples. In the present work, the molar ratio n_{MOD}/n_{Al} is much larger, due to the lower Al amount, and a distinct decrease in the ratio between BO and NBO is observed from sample A to sample C, hence a smaller polymerization degree. Additional information about the geometry of connectivity in the network can be found by looking at the distribution of Si−O−Si angles in Figure 6: an

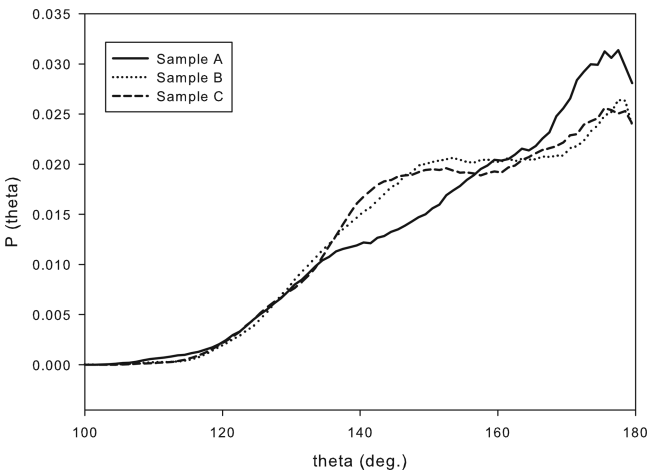

Figure 6. Si−O−Si angle distribution.

increase in Na content causes a decrease of the Si−O−Si angle, that is, a decrease in the number of tetrahedra that compose the polyhedral ring, thus a less-polymerized structure.[5]

These indications about oxygen sharing are known to be strongly correlated to some properties of glasses: for example, a loss of connectivity between tetrahedra causes a decrease in viscosity, with a consequent decrease in the energy required for atomic movements, and resulting in a lower glass transition temperature.[6] On the basis of the structural network observed after EPSR simulations, especially in terms of BO and NBO distributions, the highest glass transition temperature should be expected for sample A because of the highest tetrahedral connectivity among the investigated samples.

CONCLUSIONS

Although the presence of 5 chemical elements that correspond to 15 partial distribution functions, the combination of neutron and X-ray diffraction within the constrained EPSR modeling procedure was able to provide a reasonable and coherent structural model of these systems. Silicon and aluminum maintain their network-forming role, and their structural network is the same (for silicon) or similar (for aluminum) to their traditional behavior. Conversely, calcium and sodium, which are considered as network modifiers, are characterized by a more disordered distribution of bonding angles and coordination numbers. The increased presence of sodium in sample C corresponds to a larger number of NBO and BO″ atoms, in agreement with the charge-compensating role of sodium. As the results for these simplified glasses were more than encouraging, a more complete study is under development, introducing EXAFS measurements on Ca K-edge as a complementary technique for these same glasses, and a more complex chemical environment for the next total scattering experiments (by adding Zn and K).

AUTHOR INFORMATION

Corresponding Author
*E-mail: monica.dapiaggi@unimi.it.

Notes
The authors declare no competing financial interest.

ACKNOWLEDGMENTS

The authors thank the ISIS spallation neutron source for beam time allocation under experiment RB110004, and for X-ray data collection. We would like to thank all the people that helped us, in particular, Prosimet SpA Laboratories for their help with sample preparation, Alex Hannon for pycnometer measurements, and Emma Barney for X-ray total scattering data collection.

REFERENCES

(1) Wallace, R.; Wilk, G. *Crit. Rev. Solid State Mater. Sci.* **2003**, *28*, 231−285.
(2) Bernasconi, A.; Diella, V.; Marinoni, N.; Pavese, A.; Francescon, F. *Ceram. Int.* **2012**, *38*, 5859−5870.
(3) Konijnendijk, W.; Stevels, J. *Verres Refract.* **1976**, *30*, 371.
(4) Fluegel, A. *Glass Technol.: Eur. J. Glass Sci. Technol., Part A* **2010**, *51*, 191−201.
(5) Cormier, L.; Ghaleb, D.; Neuville, D.; Delaye, J.; Calas, G. *J. Non-Cryst. Solids* **2003**, *332*, 255−270.
(6) Cormier, L.; Neuville, D.; Calas, G. *J. Am. Ceram. Soc.* **2005**, *88*, 2292−2299.
(7) Bowron, D. T. *Mater. Sci. Eng., B* **2008**, *149*, 166−170.
(8) Greaves, G. *J. Non-Cryst. Solids* **1985**, *71*, 203−217.
(9) Benoit, M.; Profeta, M.; Mauri, F.; Pickard, C.; Tuckerman, M. *J. Phys. Chem. B* **2005**, *109*, 6052−6060.
(10) Soper, A. *EPSRshell: A User's Guide*; ISIS Disordered Materials Group: Didcot, U.K., 2010.
(11) Sivia, D. S. *Elementary Scattering Theory for X-ray and Neutron Users*; Oxford University Press: Oxford, U.K., 2012.
(12) Cormier, L.; Neuville, D. *Chem. Geol.* **2004**, *213*, 103−113.
(13) Cormack, A.; Du, J. *J. Non-Cryst. Solids* **2001**, *293*−*295*, 283−289.
(14) Benmore, C.; Soper, A. *The SANDALS Manual*; ISIS Disordered Materials Group: Didcot, U.K., 1998.
(15) Soper, A. K. *J. Phys.: Condens. Matter* **2007**, *19*, 335206.
(16) Soper, A. K. *GudrunN and GudrunX: Programs for Correcting Raw Neutron and X-ray Diffraction Data to Differential Scattering Cross Section*; ISIS Disordered Materials Group: Didcot, U.K., 2010.
(17) Soper, A. *Phys. Rev. B* **2005**, *72*, 104204.
(18) Smith, J.; Bailey, S. *Acta Crystallogr.* **1963**, *16*, 801−811.
(19) Karlsson, C.; Zanghellini, E.; Swenson, J.; Roling, B.; Bowron, D.; Borjesson, L. *Phys. Rev. B* **2005**, *72*, 064206.
(20) Angeli, F.; Delaye, J.; Charpentier, T.; Petit, J.; Ghaleb, D.; Faucon, P. *J. Non-Cryst. Solids* **2000**, *276*, 132−144.
(21) Zotov, N.; Keppler, H. *Phys. Chem. Miner.* **1998**, *25*, 259−267.
(22) Toplis, M.; Dingwell, D.; Lenci, T. *Geochim. Cosmochim. Acta* **1997**, *61*, 2605−2612.
(23) Loewenstein, R.; Wilk, G. *Am. Mineral.* **1954**, *39*, 92−96.

NOTE ADDED AFTER ISSUE PUBLICATION

The originally published version of this article included errors in Figures 2 and 3. The figures have been corrected online, and the revised version of this article was published on January 11, 2013.